Evaluation on Aerodynamic Noise of High Speed Trains with Different Streamlined Heads by LES/FW-H/APE Method

Chaowei Li[1], Yu Chen[2], Suming Xie[1(✉)], Xiaofeng Li[1], Yigang Wang[2], and Yang Gao[3]

[1] Dalian Jiaotong University, Dalian 116028, Liaoning, China
`ck_lcw@126.com, sumingxie@163.com`
[2] Tongji University, Shanghai Automotive Wind Tunnel Center, No. 4800, Cao'an Highway, Shanghai, People's Republic of China
[3] CRRC, Changchun Railway Passenger Vehicle Co., Ltd., Changchun 130062, People's Republic of China

Abstract. Aerodynamic noise of the high speed train is essential to exterior and interior noise. Five 1:8 scaled high speed train numerical models were established. The large eddy simulation was used to obtain the body turbulent fluctuation pressure. Based on the FW-H and the APE equation, far-field noise and near-field noise were obtained respectively. The difference between the simulation results of the total sound pressure level in the far field and the wind tunnel test was less than 2.0 dB(A). Their spectrum change trends were the same, and the amplitude differences were relatively small, indicating the reliability of FW-H equation. The bogie cavity is the dominant noise source, and the OSPL of turbulent pressure level is 15 –25 dB(A) higher than that of acoustic pressure inside the bogie section. The head shape varies the flow and acoustic field of the bogie section, leading to the OSPL ranges from 77.1 dB(A) to 78.6 dB(A) in the far field.

Keywords: High speed train · Aerodynamic noise · LES · FW-H · APE method

1 Introduction

Aerodynamic noise problems accompanied by the speed-up of train system are, at present, receiving a considerable attention that should be urgently resolved [1]. The head car of high speed train (HST) is a predominant aerodynamic noise source, resulted from both field test and aero-acoustic wind tunnel test [2].

In the numerical method, the turbulent fluctuating pressure in the body area of high-speed trains are usually obtained by large eddy simulation, while the far-field noise is obtained by FW-H equation based on acoustic analogy. Zhu *et al.* [3] used Delayed Detached Eddy Simulation (DDES) and Ffowcs Williams-Hawkings (FW-H) equation to solve the unsteady flow field and far-field noise of a 1:5 simplified bogie section. It is found that a highly turbulent flow is generated within the bogie cavity and the ground

increases the noise levels. The influence of head car shape on aerodynamic noise of HSTs is not clear.

Meanwhile, the acoustic pressure is caused by the pressure fluctuation and travels at the speed of sound. The energy distribution in wavenumber domain is different between turbulent and acoustic pressure, the latter has higher receptivity to transmit through the train body. Ewert *et al.* [4] deduced Acoustic Perturbation Equation (APE) to simulate the flow-induced sound field, and then it was applied to predict the sound generated by a cylinder in a cross flow. The turbulent fluctuating pressure and near field acoustic pressure are both excitations for interior noise, it is necessary to obtain near field acoustic pressure by APE.

In present study, aerodynamic noise generated by HST models with five different streamlined head was studied by Large Eddy Simulation (LES)/FW-H/APE method. The effects of head car shape to far field noise, turbulent pressure fluctuation level and acoustic pressure level in the near field were studied.

2   Methodology

The differences between real case and model case on aerodynamic noise are: Firstly, the Reynolds number effect; Secondly, the moving ground effect. There are scaling law of aerodynamic noise for the simple geometry, like the circular cylinder in free space. For the complex geometry like the HST, Lauterbach *et al.* [5] found that noise from the first bogie section can be characterized by cavity mode excitation, and it reveal only a weak Reynolds number dependence. The moving ground effect is still unclear according to published papers, because moving ground will generate additional background noise. As a result, the scaled train model and stationary ground condition were studied in this paper.

Numerical simulations are carried out using computational fluid dynamics and computational aeroacoustics method. HSTs operate at Mach number 0.2–0.3. Thus, the compressibility effects could be neglected [6]. The simulation was performed using the commercial software STAR-CCM+.

2.1   Large Eddy Simulation

To obtain unsteady flow field, Large Eddy Simulation is adapted. It is an inherently transient technique in which the large scales of the turbulence are resolved everywhere in the flow domain, and the small-scale motions are modeled.

Turbulent viscosity was modeled by WALE (Wall-Adapting Local-Eddy Viscosity) Subgrid Scale model. It uses a novel form of velocity gradient tensor in its formulation. This model is less sensitive to the value of model coefficient than the Smagorinsky model. Besides, it does not require any form of near-wall-damping, which automatically gives accurate scaling at walls. It is one of the most widely used turbulence models in recent years.

2.2 FW-H Equations

The near flied unsteady flow computation provides acoustic sources which are fed to FW-H equation for far field noise prediction. The solution of is based on Farassat's Formulation 1A [7]. For permeable source surfaces, it could account for the monopole, dipole and quadrupole noise sources within the permeable surfaces region. The total acoustic pressure $p'(\vec{x}, t)$, resulting from the sum of the thickness noise $p'_T(\vec{x}, t)$ and the loading noise $p'_L(\vec{x}, t)$, is defined as:

$$p'_T(\vec{x}, t) = \frac{1}{4\pi} \left\{ \int_{f=0} [\frac{\rho_0(\dot{U}_n + U_{\dot{n}})}{r(1 - M_r)^2}]_{ret} dS + \int_{f=0} [\frac{\rho_0 U_n (r\dot{M}_r + c(M_r - M^2))}{r^2(1 - M_r)^3}]_{ret} dS \right\} \tag{1}$$

$$p'_L(\vec{x}, t) = \frac{1}{4\pi} \frac{1}{c} \int_{f=0} [\frac{\dot{L}_r}{r(1 - M_r)^2}]_{ret} dS + \frac{1}{4\pi} \int_{f=0} [\frac{L_r - L_M}{r^2(1 - M_r)^2}]_{ret} dS$$
$$+ \frac{1}{4\pi} \frac{1}{c} \int_{f=0} [\frac{L_r(r\dot{M}_r + c(M_r - M^2))}{r^2(1 - M_r)^3}]_{ret} dS \tag{2}$$

where $L_r = \vec{L} \cdot \vec{r} = L_i \cdot r_i$, $U_n = \vec{U} \cdot \vec{n} = U_i \cdot n_i$, $\vec{r}$ and $\vec{n}$ are the direction of sound radiation and normal vector of the permable source surface respectively.

2.3 Acoustic Perturbation Equations

APE, which solves the flow-induced noise on the basis of unsteady flow simulation, was selected for the acoustic pressure calculation. The equations were firstly proposed in the terms of perturbation pressure p' and irrotational perturbation velocity u^a, and then acoustic pressure p^a was given as [4]

$$\frac{1}{c^2} \frac{\partial^2 p^a}{\partial t^2} + \frac{2\overline{U}}{c^2} \cdot \nabla \frac{\partial p^a}{\partial t} + \frac{(\overline{U} \cdot \nabla)}{c^2} (\nabla \cdot \overline{U} p^a) - \nabla^2 \left(p^a + \tau \frac{\partial p^a}{\partial t}\right)$$
$$= -\left(\frac{\bar{p}}{c^2} \frac{\partial^2 P'}{\partial t^2} + \frac{2(\overline{U} \cdot \nabla)}{c^2} \bar{\rho} \frac{\partial P'}{\partial t} + \frac{(\overline{U} \cdot \nabla)}{c^2} (\nabla \cdot \overline{U} P')\right) \tag{3}$$

where $P' = P - P_{mean}$ represents the flow field pressure fluctuation, τ is the damping term, p^a is acoustic pressure. Therefore, from the LES derived pressure fluctuation, APE can be calculated to solve the term of p^a.
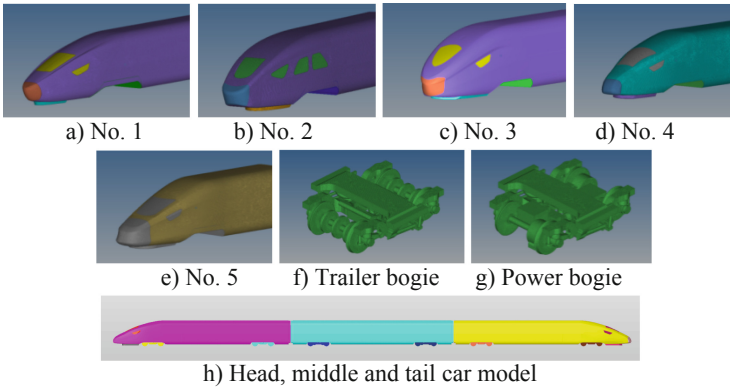
2.4 Mesh Setup

Five head cars and bogies CAD model were shown in Fig. 1. The power bogies were installed on middle car. The trailer bogies were installed on the head and tail car. The surface mesh sizes of train body and bogies range from 2 mm–4 mm.
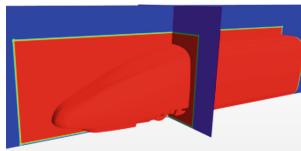
Inside the noise zone, certain requirements have to meet for correct calculation of LES and APE. The Point per Wavelength (PPW) was defined as:

$$PPW = \frac{\lambda}{\Delta x} \tag{4}$$

where λ is the wavelength of interest and Δx is the mesh size. For the frequency of 3500 Hz and mesh size of 3 mm, the corresponding PPW = 32. PPW > 30 can be regarded as a satisfied standard. Trimmer mesh, which is mainly hexahedral cell, was used to fill the volume of computational region. The cell number is about 44 million. The details were shown in Table 1. In this study, the grid number of different heads range from 44 million to 46 million, which is the numerical results are comparable.

a) No. 1   b) No. 2   c) No. 3   d) No. 4

e) No. 5   f) Trailer bogie   g) Power bogie

h) Head, middle and tail car model

Fig. 1. Five different streamlined head car, bogies and train model

Fig. 2. Noise zone and noise source weighting

Table 1. Details of mesh setup

Cell size (mm)				First prism layer height (mm)			Number of prism layer		
Noise zone	Head region	Near train	Boundary	Body	Bogies	Ground	Body	Bogies	Ground
3	6	12	48	0.015	0.015	0.35	12	12	2

2.5   Calculation Setup

The 1:8 scaled models was 10.2 m in length, 0.44 m in width and 0.5 m in height. The model was placed in a block-like computational region, with a height of 2.5 m, length of 18.7 m and width of 5.5 m, as shown in Fig. 3. The incoming velocity is 250 km/h and the turbulence intensity is 0.2%. The pressure outlet is 0 Pa. The side and top boundaries was defined as inviscid wall. The train, bogies and ground were defined as viscid wall boundary condition, which are constant to the wind tunnel test. In calculation of APE, the inlet, outlet and inviscid wall were all defined as acoustically non-reflected boundary. The non-linear aerodynamic sources around the train were enclosed by the permeable source surface.
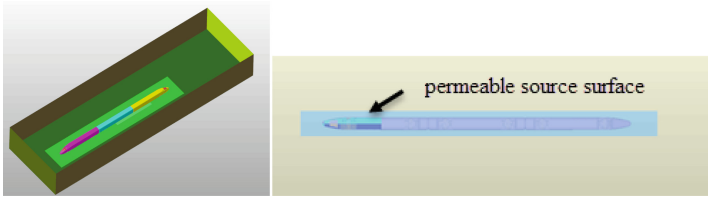

Fig. 3. Computational region and permeable source surface

The time-step size must be small enough to maintaining the proper value of acoustic CFL, defined as

$$Acoustic\ CFL = \frac{c_0 \Delta t}{\Delta x} \tag{5}$$

where c_0 is sound speed. The target of acoustic CFL is under the value of 6. Therefore, the size of time-step is set as 0.00005 s. This size corresponds to the acoustic CFL of 5.67 for the case, while ensure 10 steps inside a fluctuation cycle up to 5000 Hz. For the CFD solver, the temporal discretization scheme is second order. Normally, the spatial discretization for LES is bounding central differencing. As for the APE solver, the temporal and spatial discretization schemes are both second order.

The noise weighted function defined as Fig. 2. Inside the noise zone the value is 1. While outside the noise zone the value is 0, which means no sound would be produced there. In the transition band, with a thickness of 15 mm, a spatial Hanning window was applied to enable the smooth variation between 0 to 1. The noise damping function, which contributes to the term τ in Eq. 3, is the opposite of the noise weighted function. It has the value of 0 inside the noise zone and the value of 1 outside the noise zone.

Firstly, the RANS model SST k-ω was run to initialize the unsteady flow. Then LES started for a relatively large time-step of 0.0005 s, with the duration time of 0.5 s, which is roughly two times the flow-through time of the whole region or 60 times the flow-through time of the first bogie section. Hence, the time-step switched to 0.00005 s and ran for 1000 steps. According to APE, averaged pressure should be solved before APE calculation started. Therefore, averaged pressure has been recording 750 steps prior APE activated. The data sampling began after APE had run for 250 steps. During 2500 steps data sampling, flow field pressure obtained from LES and acoustic pressure obtained from APE were recorded.

2.6   Aeroacoustic Wind Tunnel Test

The experiment was carried out in the SAWTC aeroacoustic wind tunnel at Tongji University, where the background noise level is 72.4 dB(A) at the nozzle speed of 250 km/h. The wind tunnel is a 3/4 open section wind tunnel with a nozzle size of 6.0 m × 4.25 m, the turbulence intensity is 0.2%. The nozzle speed in the experiment is the same as the inlet velocity of simulation.

The wind test model is the same with No. 4. The train model is made of stiff wood and the exterior surfaces were processed Computerized Numerical Control (CNC). The bogies were made of ABS Engineering Plastics. Figure 4 shows a general view of the train model in aeroacoustic wind tunnel. The test model is the same with No. 4. The model was attached above a reflective ground. It was mounted on simplified rails, and the head car nose was 1 m away from the nozzle. The ground clearance between the train body and the ground 53 mm, which is 1/8 of a real HST ground clearance also. This relative movement can be simulated in wind tunnel tests using a moving belt under the train, but this has not been used here as it would generate additional background noise.

Three B&K free field microphones are located 7.5 m away from the center line of the train, and 0.8 m in height. The distances between F1, F2 and F3 are 3 m. The sampling frequency and sampling time of microphones are 48 kHz and 10 s respectively. Figure 5 shows the spectrum of the background noise and train model.
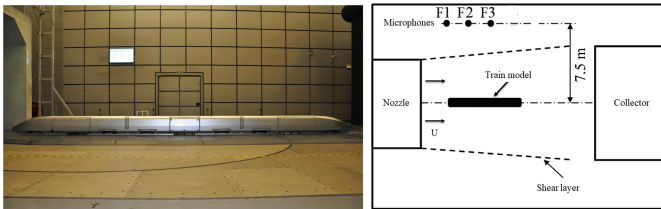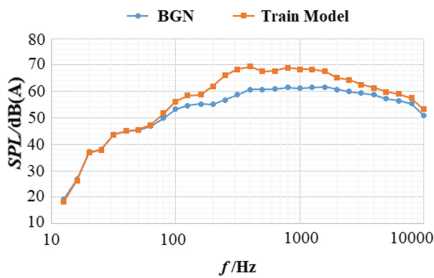

Fig. 4. Wind tunnel test scheme

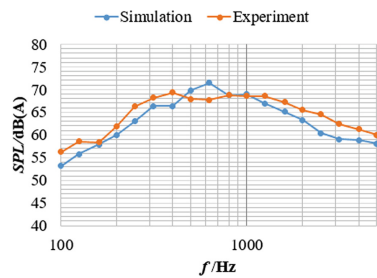**Fig. 5.** Background noise and train model noise

Fig. 6. 1/3 Octave band spectrum of F2

3   Results and Discussion

3.1   Validation of Simulation and Experiment

Due to a high background noise level in the low frequency range generated from the nozzle itself, simulation results are only considered above 100 Hz. The background

noise of the anechoic chamber was also shown. Its noise level was by several orders of magnitude lower than those generated from the HST model in the frequency range between 100 Hz and 3500 Hz.

Figure 6 shows the spectrum of F2 obtained by wind tunnel test and numerical simulation. The numerical simulation results are consistent with the wind tunnel test results, and the amplitude is not very different. The amplitude of the SPL is 60 dB (A) in the lower and higher frequency bands. The amplitude of the SPL is 65–70 dB (A) in the middle frequency band (300 Hz–2000 Hz). There is no peak in the whole frequency band, indicating that the far-field noise is broadband noise.

The total SPL of each microphone are shown in Table 2. The differences between each microphone are within 2 dB(A). The results of simulation are consistent with those of wind tunnel test, which shows that the prediction of far-field noise based on FW-H equation is basically correct.

Table 2. Total sound pressure level of test points dB(A)

Items	F1	F2	F3
Simulation	78.5	78.4	80.6
Test	78.1	78.7	78.6
Δ(Simulation-Test)	0.4	−0.3	2.0

### 3.2 Influence of Head Shape on Pressure and Acoustic in the Near Field

The simplified model does not reflect every single feature of a real train. For aerodynamic noise studies, any component like air-condition inlets, wiper of head car, and small antennas are important noise sources. However, the simplified train and bogie models reflects the most important noise sources.

Compared with the background noise, the HST aerodynamic noise energy was mainly between 100 Hz to 3500 Hz. The Overall SPL in A-weighting was obtained for both turbulent pressure (TP) and acoustic pressure (AP) from 100 Hz to 3500 Hz. The contours of OSPL were shown in Fig. 7 and 8.

The distribution of TP level and AP level are similar for five heads. Both of them are much higher on the underbody structures. The OSPL of TP level is 15–25 dB(A) higher than that of AP inside the bogie section. The TP is strong in the rear edge of bogie cavity, cowcatcher and wheels, while it is weak in the top roof of bogie cavity. The AP is strong in the rear edge and top roof of bogie cavity. The vortex interaction between shear layer and rear edge of bogie cavity are not only the major source of TP, but also the major one of AP.

3.3 Influence of Head Shape on Far Field Noise

Table 3 shows the SPL of F2 in the far field. The OSPL ranges from 77.1 dB(A) to 78.6 dB(A), which means the different styling of head car affects the SPL in the far field.
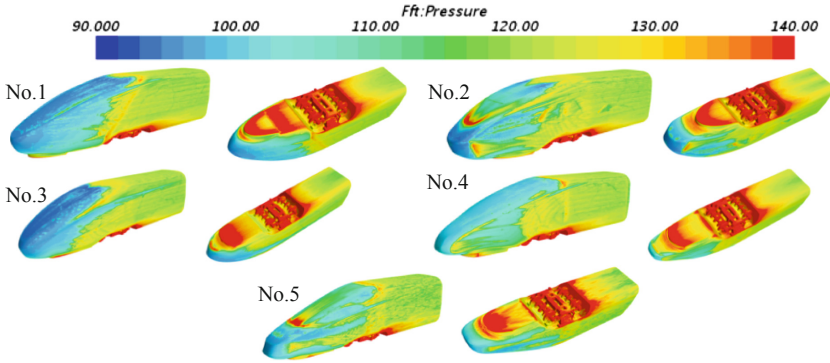
Fig. 7. Turbulent pressure fluctuation level obtained by LES dB(A)
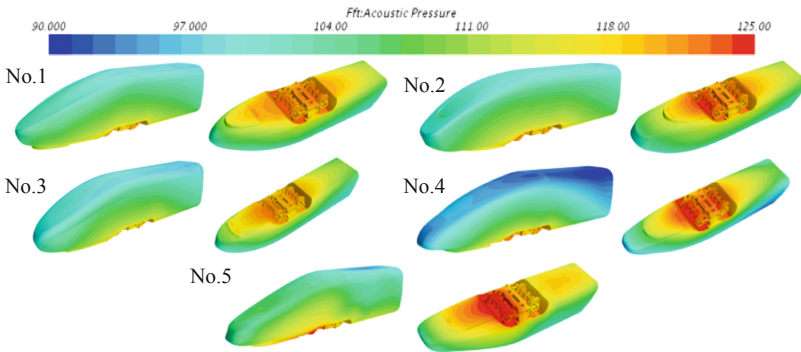
Fig. 8. Acoustic pressure level obtained by APE dB(A)

The turbulent and acoustic pressure levels on the upper head are much lower than that of underbody structure. That is to say, the head shape varies the flow and acoustic field of the first bogie section.

Table 3. Sound pressure level in the far field dB(A)

SPL	No. 1	No. 2	No. 3	No. 4	No. 5
F2	77.9	77.1	77.5	78.4	78.6

Figure 9 gives the spectrum in the far field. The trends of five streamlined head are similar. The No. 5 HST emits higher noise level in the frequency range 500 Hz–1000 Hz. The No. 2 and No. 3 HSTs have lower noise level in the frequency range 200 Hz–1250 Hz.
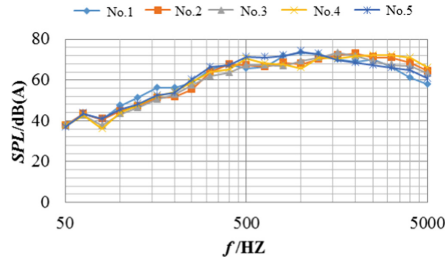
Fig. 9. The spectrum of F2

4 Conclusion

Hybrid LES/FW-H/APE methods were performed to investigate the aerodynamic noise of HSTs with five different streamlined heads. The No.4 HST with the same configuration was researched experimentally in the aeroacoustic wind tunnel at SAWTC. The SPL in the far field obtained by LES/FW-H was validated by the experimental measurement and it provided good agreement. The acoustic pressure gives the insight that the acoustic pressure is strong in the rear edge and top roof of bogie cavity, and different from the turbulent pressure level distribution.

The OSPL of turbulent pressure level is 15–25 dB(A) higher than that of acoustic pressure for every same place inside the bogie section. The different shapes of head car affect the underbody flow field, leading to the differences of SPL in the far field, turbulent and acoustic pressure level in the near field.

References

1. Thompson, D.: Railway Noise and Vibration: Mechanisms, Modeling and Means of Control. Elsevier, Amsterdam (2009)
2. Thompson, D., Iglesias, E., Liu, X., et al.: Recent developments in the prediction and control of aerodynamic noise from high-speed trains. Int. J. Rail Transp. **3**(3), 119–150 (2015)
3. Zhu, J., Hu, Z., Thompson, D.: The effect of a moving ground on the flow and aerodynamic noise behaviour of a simplified high-speed train bogie. Int. J. Rail Transp. **5**(2), 110–125 (2017)
4. Ewert, R., Wolfgang, S.: Acoustic perturbation equations based on flow decomposition via source filtering. J. Comput. Phys. **188**(2), 365–398 (2003)
5. Lauterbach, A., Ehrenfried, K., Loose, S., et al.: Microphone array wind tunnel measurements of Reynolds number effects in high-speed train aeroacoustics. Int. J. Aeroacoust. **11**(3 & 4), 411–446 (2012)
6. Ask, J., Davidson, L.: An acoustic analogy applied to the laminar upstream flow over an open 2D cavity. Comptes Rendus Mécanique **333**(9), 660–665 (2005)
7. Brenter, K., Farassat, F.: An analytical comparison of the acoustic analogy and Kirchhoff formulation for moving surfaces. AIAA J. **36**(8), 1379–1386 (1998)